

Four electrons in a two-leg Hubbard ladder: Exact ground states.

Endre Kovács and Zsolt Gulácsi

Department of Theoretical Physics, University of Debrecen, H-4010 Debrecen, Hungary

(Dated: February 6, 2008)

Abstract

In the case of a two-leg Hubbard ladder we present a procedure which allows the exact deduction of the ground state for the four particle problem in arbitrary large lattice system, in a tractable manner, which involves only a reduced Hilbert space region containing the ground state. In the presented case, the method leads to nine analytic, linear, and coupled equations providing the ground state. The procedure which is applicable to few particle problems and other systems as well is based on an \mathbf{r} -space representation of the wave functions and construction of symmetry adapted orthogonal basis wave vectors describing the Hilbert space region containing the ground state. Once the ground state is deduced, a complete quantum mechanical characterization of the studied state can be given. Since the analytic structure of the ground state becomes visible during the use of the method, its importance is not reduced only to the understanding of theoretical aspects connected to exact descriptions or potential numerical approximation scheme developments, but is relevant as well for a large number of potential technological application possibilities placed between nano-devices and quantum calculations, where the few particle behavior and deep understanding are important key aspects to know.

PACS numbers: PACS No. 71.10.Fd, 71.27.+a, 73.21.-b

I. INTRODUCTION

In condensed matter context, in experiments or related theoretical interpretations we often encounter small number of particles confined in a system or device, for example, in the case of quantum dots¹, quantum well structures², mesoscopic systems³, experimental entanglement⁴, micro-crystals⁵, cold gases trapped in optical lattices^{6,7}, optical bound states⁸, segregation⁹, interfacial stress and fracture¹⁰, self organized structures¹¹, sintering¹², or compounds studied in the low concentration limit¹³. Such problems, presenting both theoretical^{14,15,16,17} and technological^{9,10,12,18,19,20} interest have continuously attracted increasing attention. Starting from even one electron problems solved exactly¹⁷, several cases of interest for two^{21,22,23,24,25,26}, three^{14,15,27,28,29}, four^{30,31,32}, or few^{33,34,35} particles have been studied, concentrating on the model behavior in the low concentration limit, or motivated by experimentally measured characteristics. In this hierarchy of the increasing number of carriers in the study of a given problem, the particle number four ($N_p = 4$) represents a special case, since it is close to the particle number limit around which one can hope that deep rigorous descriptions can be made³⁶ even in the non-integrable cases, the problem is also treatable from the numerical side as well³⁷, statistics and $T \neq 0$ characterization can be given³⁸, and the problem retain even many-body aspects of the system's behavior^{39,40,41}.

The simulations on the $N_p = 4$ particle problem started more than a decade ago^{37,42}, but up today, only few valuable results are known in this subject in the condensed matter context, as follows. The energy dependence of the maximal Lyapunov exponent has been studied for 1D Lenard-Jones system⁴³, the spinless fermion case has been analyzed as a simplified model for correlated electrons^{30,31}, the conjecture of the Andreev-Lifshitz supersolid has been studied³², entangled states have been described in the high frequency region⁴⁴, doped quantum well structures have been investigated², special cases where only two pairs of particles interact on a lattice were considered⁴⁵, localization lengths have been estimated in 1D disordered systems³, and the behavior in the presence of Coulomb forces has been analyzed⁴⁶. As can be seen, the knowledge accumulated in this direction is relatively poor. Approximated procedures have been applied in different conditions for different systems of interest, but the level of exact characteristics has not been reached yet.

The need to study at exact level system holding $N_p = 4$ particles is enhanced by several motivations. First of all, $N_p = 4$ it is placed in the low density limit, and as known, in this

limit, especially in low dimensions, no class of diagrams can be neglected in describing the system⁴⁷. Given by this difficulty, one often finds that traditional approximation schemes which work at higher densities, here fail⁴⁸ or provide unphysical results⁴⁹. Secondly, we are placed in the concentration limit where the formation of Fermi liquid properties can be studied³⁰, and since this parameter region is usually numerically accessible, research with analytical focus, starting from numerical results, also can be done. Thirdly, as several times has been accentuated^{50,51}, key aspects of the unapproximated descriptions are often hidden in the few particle cases. The four particle case seems to be tractable also from this point of view. Finally, in $N_p = 4$ case we face a situation which experimentally is produced, having potential application possibilities in several areas, as for example in the study of entangled states⁵², non-local character of quantum theory⁵³, high precision spectroscopy⁵⁴, quantum communication, quantum cryptography, and quantum computation⁵⁵, fields where deep and high quality results are clearly demanded⁵⁷.

Starting from the motivations presented above, we show in this paper that for the $N_p = 4$ case, exact, analytical, and explicit results holding essential information about the system behaviour can be indeed provided, even for arbitrary large systems. To show this, we present below the exact ground state for four interacting electrons placed in an arbitrary large two leg Hubbard ladder described by periodic boundary conditions. This is given in conditions for which, even the known three (quantum mechanical) particle exact results are very rare for systems taken outside of one dimension (see Ref.^[29] and the references therein), hence we hope that the presented results will generate creative advancements.

In order to obtain such results, a direct space representation is used for the wave functions. Starting from local particle configurations, symmetry adapted ortho-normalized basis wave vectors are constructed. Based on these, in the studied case, an explicit and analytic closed system of 9 equations is constructed, whose secular equation provides the ground state wave function and energy. Deducing the ground state wave function for different microscopic parameters of the model, ground state expectation values are calculated for different physical quantities of interest, and correlation functions are deduced in order to characterize the ground state properties.

The method which is described here is in principle not model or particle number dependent, and could be applied for other systems as well. In presenting our calculations, the aim was not to hide the obtained results behind a numerical treatment or deduced symmetry

properties, (which certainly also can be done), but to show clear, visible, and explicit properties which, based on the provided essential characteristics, could enhance further creative thinking or applications. In order to underline the importance of these aspects we note for example, that in recent studies made for states containing 2-4 particles, especially in attempts to characterize the entanglement⁵², or quantum dots⁵⁶, often the analysis must be made without to know the state completely^{57,58}. We show below how such ingredients, at least at the level of the ground state, are possible to overcome.

The remaining part of the paper is structured as follows. Section II. presents the Hamiltonian, the deduction procedure and the ground state wave functions, Section III. exemplifies the physical properties of the ground state, Sect. IV. presents the summary and conclusions of the paper, while the Appendices A - B presenting mathematical details, close the presentation.

II. HAMILTONIAN AND GROUND STATE WAVE FUNCTIONS.

The strategy which we use for presentation is the following one. We have chosen a simple model which allow us to characterize the construction of exact ground states in the presence of four particles. After presenting the results we indicate how the procedure could be applied for other systems as well.

A. Presentation of the Hamiltonian

The Hamiltonian we use for presentation has the form of a standard two-leg Hubbard ladder Hamiltonian

$$\hat{H} = -t_{\parallel} \sum_{\langle i,j \rangle_{\parallel}, \sigma} (\hat{c}_{i,\sigma}^{\dagger} \hat{c}_{j,\sigma} + H.c.) - t_{\perp} \sum_{\langle i,j \rangle_{\perp}, \sigma} (\hat{c}_{i,\sigma}^{\dagger} \hat{c}_{j,\sigma} + H.c.) + U \sum_i \hat{n}_{i,\uparrow} \hat{n}_{i,\downarrow}, \quad (1)$$

where $\hat{c}_{i,\sigma}^{\dagger}$ creates an electron at site i with spin σ , t_{α} holding the index $\alpha = \parallel, \perp$ are nearest-neighbor hopping amplitudes along and perpendicular to ladder legs, U is the on-site Coulomb interaction, and $\langle i, j \rangle_{\alpha}$ represents nearest-neighbor sites in α direction taken into account in the sum over the lattice sites only once.

B. The construction of the basis wave vectors

If we would like to analyze by exact diagonalization the four particle problem in the singlet case in a two leg Hubbard ladder containing N lattice sites, we must treat numerically a Hilbert space of $d_H = [N(N-1)/2]^2$ dimensions, where for example at $N = 30$ we have $d_H = 2.16 \cdot 10^5$, and for $N \rightarrow \infty$ one encounters $d_H \rightarrow \infty$ as $d_H \sim N^4$.

We show below how it is possible to deduce exactly the ground state for a such type of system in the case of an arbitrary large two leg Hubbard ladder based on only nine linear and analytic equations, and to extract essential information from the obtained results. In order to do this, first of all we delimit exactly the Hilbert space region (\mathcal{H}_g) containing the ground state by the construction of nine type of orthogonal basis wave vectors spanning \mathcal{H}_g . This procedure is presented below.

1. The generating configurations

We are interested first to have an image about the possible type of states of the studied four particles in the system under consideration. To obtain such type of information, we number all lattice sites of the ladder as shown in Fig.1 (periodic boundary conditions are considered). In the figure, N , considered even number, denotes the number of sites within the system, while $n = N/2$ gives the number of rungs, respectively. Using now an \mathbf{r} -space representation, one observes that since the ladder legs, and the spin reversed configurations are equivalent, the studied four particles can be placed into the system only in nine possible ways, as depicted in Fig.2. The presented possibilities, denoted by capital letters A to J will provide nine type of basis wave vectors (denoted by the same letters), whose construction is presented below. We mention that the subscripts i, j, k are denoting particle positions within the considered states A to J presented in Fig.2, which are such chosen, to have the first particle position placed into the origin (e.g. lattice site 1). In the following, the nine possible four-particle states presented in Fig.2 will be called *generating configurations*. How one arrives from the generating configuration $X = A, B, \dots, J$ to the base vector $|X\rangle$, is explained in the following two subsections.

2. The sum of configurations related to each generating configuration

Each generating configuration provides other seven related configurations (brother configurations) of the same type. These are obtained by a) rotating the generating configuration by 180 degrees along the longitudinal symmetry axis of the ladder, b) rotating the generating configuration by 180 degrees along the symmetry axis perpendicular to the ladder, c) rotating by 180 degrees the configuration obtained at b) along the longitudinal symmetry axis of the ladder, and finally, d) other four related configurations are obtained by reversing all spin orientations in the generating configuration and the configurations deduced at points a)-c). As an example, the eight related configurations describing the state $D_{i,j}$ taken at $i = 2, j = 3$, are depicted in the first column of Fig.3.

After this step, since all lattice sites are equivalent, the different „related” configurations are translated by *elementary translation* $N/2$ times along the ladder, and all the contributions are added. We obtain in this manner a sum of configurations for each generating configuration. Such a sum contains $8 \times N/2$ components. For example, in the case of the $D_{2,3}$ state, this sum is presented in Fig.3.

The procedure described above must be effectuated separately for each generating configuration. As a result, we obtain at this point nine configuration sums. Each of these sums will give rise to one basis wave vector as follows.

3. The basis wave vectors

A given configuration sum described in the previous subsection provides one basis wave vector if each individual configuration of the sum is written in mathematical form via four creation operators acting on the bare vacuum. In order to do this, we have to fix the order of creation operators for each type of contribution, which has been done as follows. For two doubly occupied sites we write the creation operators of the couples next to each other, first the spin up, then the spin down contribution, as $\hat{c}_{i,\uparrow}^\dagger \hat{c}_{i,\downarrow}^\dagger \hat{c}_{j,\uparrow}^\dagger \hat{c}_{j,\downarrow}^\dagger |0\rangle$, where only the restriction $i \neq j$ exists. In the case of basis wave vectors containing only one doubly occupied site at i one uses $\hat{c}_{i,\uparrow}^\dagger \hat{c}_{i,\downarrow}^\dagger \hat{c}_{j,\uparrow}^\dagger \hat{c}_{k,\downarrow}^\dagger |0\rangle$, where $i \neq j$ and $i \neq k$ must hold. Finally, for cases without double occupancies, the convention $\hat{c}_{i,\uparrow}^\dagger \hat{c}_{j,\uparrow}^\dagger \hat{c}_{k,\downarrow}^\dagger \hat{c}_{l,\downarrow}^\dagger |0\rangle$ is considered, where $i < j$, and $k < l$ must hold. Using these conventions, for example, in the case of $|D_{i,j}\rangle$, taken at $i = 2, j = 3$ and depicted

in Fig.3. the result becomes

$$\begin{aligned}
|D_{2,3}\rangle = & ((\hat{c}_{1\uparrow}^\dagger \hat{c}_{1\downarrow}^\dagger \hat{c}_{2\uparrow}^\dagger \hat{c}_{(n+3)\downarrow}^\dagger + \hat{c}_{2\uparrow}^\dagger \hat{c}_{2\downarrow}^\dagger \hat{c}_{3\uparrow}^\dagger \hat{c}_{(n+4)\downarrow}^\dagger + \hat{c}_{3\uparrow}^\dagger \hat{c}_{3\downarrow}^\dagger \hat{c}_{4\uparrow}^\dagger \hat{c}_{(n+5)\downarrow}^\dagger + \dots) \\
& + (\hat{c}_{1\uparrow}^\dagger \hat{c}_{1\downarrow}^\dagger \hat{c}_{(n+3)\uparrow}^\dagger \hat{c}_{2\downarrow}^\dagger + \hat{c}_{2\uparrow}^\dagger \hat{c}_{2\downarrow}^\dagger \hat{c}_{(n+4)\uparrow}^\dagger \hat{c}_{3\downarrow}^\dagger + \hat{c}_{3\uparrow}^\dagger \hat{c}_{3\downarrow}^\dagger \hat{c}_{(n+5)\uparrow}^\dagger \hat{c}_{4\downarrow}^\dagger + \dots) \\
& + (\hat{c}_{(n+1)\uparrow}^\dagger \hat{c}_{(n+1)\downarrow}^\dagger \hat{c}_{(n+2)\uparrow}^\dagger \hat{c}_{3\downarrow}^\dagger + \hat{c}_{(n+2)\uparrow}^\dagger \hat{c}_{(n+2)\downarrow}^\dagger \hat{c}_{(n+3)\uparrow}^\dagger \hat{c}_{4\downarrow}^\dagger + \hat{c}_{(n+3)\uparrow}^\dagger \hat{c}_{(n+3)\downarrow}^\dagger \hat{c}_{(n+4)\uparrow}^\dagger \hat{c}_{5\downarrow}^\dagger + \dots) \\
& + (\hat{c}_{(n+1)\uparrow}^\dagger \hat{c}_{(n+1)\downarrow}^\dagger \hat{c}_{3\uparrow}^\dagger \hat{c}_{(n+2)\downarrow}^\dagger + \hat{c}_{(n+2)\uparrow}^\dagger \hat{c}_{(n+2)\downarrow}^\dagger \hat{c}_{4\uparrow}^\dagger \hat{c}_{(n+3)\downarrow}^\dagger + \hat{c}_{(n+3)\uparrow}^\dagger \hat{c}_{(n+3)\downarrow}^\dagger \hat{c}_{5\uparrow}^\dagger \hat{c}_{(n+4)\downarrow}^\dagger + \dots) \\
& + (\hat{c}_{3\uparrow}^\dagger \hat{c}_{3\downarrow}^\dagger \hat{c}_{2\uparrow}^\dagger \hat{c}_{(n+1)\downarrow}^\dagger + \hat{c}_{4\uparrow}^\dagger \hat{c}_{4\downarrow}^\dagger \hat{c}_{3\uparrow}^\dagger \hat{c}_{(n+2)\downarrow}^\dagger + \hat{c}_{5\uparrow}^\dagger \hat{c}_{5\downarrow}^\dagger \hat{c}_{4\uparrow}^\dagger \hat{c}_{(n+3)\downarrow}^\dagger + \dots) \\
& + (\hat{c}_{3\uparrow}^\dagger \hat{c}_{3\downarrow}^\dagger \hat{c}_{(n+1)\uparrow}^\dagger \hat{c}_{2\downarrow}^\dagger + \hat{c}_{4\uparrow}^\dagger \hat{c}_{4\downarrow}^\dagger \hat{c}_{(n+2)\uparrow}^\dagger \hat{c}_{3\downarrow}^\dagger + \hat{c}_{5\uparrow}^\dagger \hat{c}_{5\downarrow}^\dagger \hat{c}_{(n+3)\uparrow}^\dagger \hat{c}_{4\downarrow}^\dagger + \dots) \\
& + (\hat{c}_{(n+3)\uparrow}^\dagger \hat{c}_{(n+3)\downarrow}^\dagger \hat{c}_{(n+2)\uparrow}^\dagger \hat{c}_{1\downarrow}^\dagger + \hat{c}_{(n+4)\uparrow}^\dagger \hat{c}_{(n+4)\downarrow}^\dagger \hat{c}_{(n+3)\uparrow}^\dagger \hat{c}_{2\downarrow}^\dagger + \hat{c}_{(n+5)\uparrow}^\dagger \hat{c}_{(n+5)\downarrow}^\dagger \hat{c}_{(n+4)\uparrow}^\dagger \hat{c}_{3\downarrow}^\dagger + \dots) \\
& + (\hat{c}_{(n+3)\uparrow}^\dagger \hat{c}_{(n+3)\downarrow}^\dagger \hat{c}_{1\uparrow}^\dagger \hat{c}_{(n+2)\downarrow}^\dagger + \hat{c}_{(n+4)\uparrow}^\dagger \hat{c}_{(n+4)\downarrow}^\dagger \hat{c}_{2\uparrow}^\dagger \hat{c}_{(n+3)\downarrow}^\dagger + \hat{c}_{(n+5)\uparrow}^\dagger \hat{c}_{(n+5)\downarrow}^\dagger \hat{c}_{3\uparrow}^\dagger \hat{c}_{(n+4)\downarrow}^\dagger + \dots))|0\rangle
\end{aligned}$$

Similar procedure applies for all basis wave vectors. We mention that the so obtained basis wave functions are orthogonal.

Here we must note that because of the fixed conventions presented above, sometimes an additional negative sign arises in the process of writing the mathematical expression corresponding to a basis wave vector component translated from the end to the beginning of the ladder in the presence of the periodic boundary conditions. For example, if we translate the vector $\hat{c}_{1,\uparrow}^\dagger \hat{c}_{N/2,\uparrow}^\dagger \hat{c}_{2,\downarrow}^\dagger \hat{c}_{3,\downarrow}^\dagger |0\rangle$ by an elementary translation along the ladder, according to the fixed conventions one obtains $\hat{c}_{2,\uparrow}^\dagger \hat{c}_{1,\uparrow}^\dagger \hat{c}_{3,\downarrow}^\dagger \hat{c}_{4,\downarrow}^\dagger |0\rangle = -\hat{c}_{1,\uparrow}^\dagger \hat{c}_{2,\uparrow}^\dagger \hat{c}_{3,\downarrow}^\dagger \hat{c}_{4,\downarrow}^\dagger |0\rangle$.

C. The ground state wave function

After the calculation presented above, we are in the possession of nine type of orthogonal basis wave vectors $|A_i\rangle, |B_i\rangle, \dots, |J_{i,j,k}\rangle$, enumerated together with their generating configuration in Fig.2. Let us denote these basis wave vectors by $|O_{i,j,\dots}^{(m)}\rangle$, $m = 1, 2, 3, \dots, 9$. Now one observes that by applying the Hamiltonian on a given $|O_{i,j,\dots}^{(m)}\rangle$ basis wave vector with fixed m , we obtain the result inside the $\{|O_{i,j,\dots}^{(m)}\rangle\}$ set. Consequently, nine explicitly given analytic linear equations form a closed system of equations, whose secular equation, by its minimum eigenvalue, contains the ground state at attractive U . The nine equations are exemplified in Appendix A and are available in their complete extent in Ref.^[59]. The ground state nature of the minimum energy eigenstate has been tested by exact numerical diagonalizations taken on the full Hilbert space for different N values.

The fact that the analytic solution of the problem can be given in such a manner for arbitrary large ladder length is connected to the observation that with increasing N , the type of the particle configurations describing the system (see Fig.2), remains unchanged. The deduction of the ground state itself from the system of equations presented in Appendix A must be numerically given⁶⁰. Since the possible inter-particle distances (e.g. the possible values of the $i, j, ..$ indices in $O_{i,j,..}^{(m)}$ at fixed m) depend on the N value, the number of equations which must be numerically treated depends on N in the frame of the same analytic expressions. For example, for the $m = 1$ case we have $1 < i \leq 1 + N/4$, for the $m = 2$ case we have $1 \leq i \leq 1 + N/4$, etc. The number of obtained equations d_e is however significantly lower than d_H , the $c_g = d_H/d_e$ ratio being at least of order 10^2 at intermediate $N \sim O(10)$ values. Increasing N , c_g further increases.

D. Application possibilities in other cases

In fact, the deduced system of equations, based on symmetry properties, delimitates from the full Hilbert space a d_e dimensional space region, inside of which the ground state is placed. The deduction of a such region is possible for other (non-disordered) models, and other particle numbers as well. In order to do this, we mention that if the lattice sites are equivalent, the elementary translation of a particle configuration can be in principle given with a site independent multiplicative phase factor $\exp(i\alpha_{trans})$. Furthermore, the rotation of a particle configuration along a symmetry axis can be given in principle with a multiplicative phase factor of the form $\exp(i\alpha_{rot})$, both $\alpha_{trans}, \alpha_{rot}$ providing their contributions in the basis wave vectors⁶¹. In the described case, we have $\alpha_{trans} = \alpha_{rot} = 0$, but in other cases, the energy can be minimized in function of these parameters.

In deducing the linear system of equations describing \mathcal{H}_g in a new case characterized by a new \hat{H} , one must start from a given basis wave vector (denoted by $|v_1\rangle$, for example). This is obtained from a generating particle configuration, which is translated and rotated as specified above, all such obtained configurations being summed up. From technical reasons, the first generating particle configuration must be such chosen to contain (for 1/2 spin fermions) only double occupied sites placed in nearest neighbor sites. Calculating now $\hat{H}|v_1\rangle$, the result becomes a linear combination containing new base vectors $|v_2\rangle, ..., |v_{n_1}\rangle$, holding the same symmetry properties, but being related to new generating configurations. Continuing the

procedure by calculating $\hat{H}|v_2\rangle, |\hat{H}|v_3\rangle$, etc., since periodic boundary conditions are used, the linear system of equations closes up. It is even not important to know all distinct particle configuration possibilities, since these are automatically generated by the $\hat{H}|v_i\rangle$ operation.

III. GROUND STATE PROPERTIES

By diagonalizing the system of equations presented in Appendix A and taking the minimum energy solution, one finds the ground state wave function $|\Psi_g\rangle$. Using this, the complete quantum mechanical characterization of the ground state can be given. In order to exemplify the results, we present in (B1,B2) explicit expressions containing the leading terms of the ground state wave function for two parameter values. Even Appendix B shows that in the leading terms of the ground state wave function, the particles have the tendency to be placed in pairs, the pairs tending to occupy the highest possible distance between them. This is reflected as well in the density-density correlation function depicted in Fig.4c.

Ground state expectation values and correlation functions are exemplified in Figs. 4-5. calculated for $N = 28$, e.g. ladder containing 14 rungs described by periodic boundary conditions taken along the ladder. The correlation functions are defined as follows. The density-density correlation function has the expression

$$C_n(r) = \frac{1}{N} \sum_{i=1}^N (\langle \hat{n}_i \hat{n}_{i+r} \rangle - \langle \hat{n}_i \rangle \langle \hat{n}_{i+r} \rangle) \quad (2)$$

where $\hat{n}_i = \hat{n}_{i\uparrow} + \hat{n}_{i\downarrow}$, $\hat{n}_{i,\sigma} = \hat{c}_{i\sigma}^\dagger \hat{c}_{i\sigma}$. The spin correlations are studied via

$$C_{S^z}(r) = \frac{1}{N} \sum_{i=1}^N (\langle \hat{S}_i^z \hat{S}_{i+r}^z \rangle - \langle \hat{S}_i^z \rangle \langle \hat{S}_{i+r}^z \rangle), \quad (3)$$

where $\hat{S}^z = (1/2)(\hat{n}_{i,\uparrow} - \hat{n}_{i,\downarrow})$. The superconducting pairing s-wave⁶² correlation function is

$$C_{sw}(r) = \frac{1}{N} \sum_{i=1}^N (\langle \hat{c}_{i\uparrow}^\dagger \hat{c}_{i\downarrow}^\dagger \hat{c}_{(i+r)\downarrow} \hat{c}_{(i+r)\uparrow} \rangle - \langle \hat{c}_{i\uparrow}^\dagger \hat{c}_{(i+r)\uparrow} \rangle \langle \hat{c}_{i\downarrow}^\dagger \hat{c}_{(i+r)\downarrow} \rangle), \quad (4)$$

and the superconducting pairing d-wave⁶³ correlations are studied via

$$C_{dw}(r) = \frac{1}{N} \sum_{i=1}^N \langle \hat{\Delta}^\dagger(i+r) \hat{\Delta}(i) \rangle \quad (5)$$

where $\hat{\Delta}(i) = (\hat{c}_{i_2\downarrow} \hat{c}_{i_1\uparrow} - \hat{c}_{i_2\uparrow} \hat{c}_{i_1\downarrow})$. The i in $\hat{\Delta}(i)$ denotes a rung connecting the lattice sites i_1, i_2 . The r values inside the figures are given in lattice constant units.

Fig.4a presents the ground state energy and the potential energy in t_{\parallel} units in function of $u = |U/t_{\parallel}|$ at $t_{\parallel} = t_{\perp}$. Fig.4b shows that the spin-spin correlations are exponentially decreasing, the decrease rate in the $\exp(-r/\xi)$ being of the form $1/\xi = 0.34 + 0.78\sqrt{|u|}$. The density-density correlations depicted in Fig.4c show that the particles tend to occupy opposite positions in the ladder closed by periodic boundary conditions.

In Fig.5 the behavior of the superconducting correlation functions is presented. In these plots $u = U/t_{\parallel}$ holds. The correlations in Fig.5 are decreasing with r , and for s -wave case slightly increase by increasing the attractive U value. Fig.5c further shows that the decrease of the inter-leg hopping amplitude at fixed on-site interaction is detrimental to d -wave pairing correlations. Similar behavior has been found also by others⁶².

IV. SUMMARY AND CONCLUSIONS

We describe a procedure which allows the exact deduction of ground state wave functions for few particles in lattice models. The main result of our paper is that indeed, a such type of analytic description can be done. In the case of an arbitrary large two leg Hubbard ladder taken with periodic boundary conditions and containing four electrons, presented in details, the method leads for the singlet state to nine analytic linear and coupled closed system of equations, whose secular equation, through its minimum eigenvalue solution, provides the ground state wave function and ground state energy. The procedure is based on a \mathbf{r} -space representation of the wave functions and properly constructed symmetry adapted orthogonal basis wave vectors. These are obtained from generating particle configurations translated and rotated in the lattice and finally added. The linear system of equations is obtained by applying the Hamiltonian on the deduced basis wave vectors. The procedure can be applied for other systems as well.

The fact that the analytic structure of the ground state becomes visible by the use of the method underlines that the presented procedure contributes not only to the understanding of theoretical aspects related to exact descriptions, or development possibilities of new numerical approximation schemes, but has implications on a broad spectrum of subfields related to technological developments placed in between nano-devices and quantum computation, where the exact knowledge of the behavior of a small number of quantum mechanical particles plays a main role.

Acknowledgments

This work was supported by the Hungarian Scientific Research Fund through contract OTKA-T-037212. The numerical calculations have been done at the Supercomputing Lab. of the Faculty of Natural Sciences, Univ. of Debrecen, supported by OTKA-M-041537.

APPENDIX A: THE LINEAR SYSTEM OF EQUATIONS CONTAINING THE GROUND STATE.

This Appendix presents the nine analytic equations describing the action of the Hamiltonian on the basis wave vectors.

The first two equations are devoted to the $|A_i\rangle, |B_i\rangle$ species containing only (two) doubly occupied sites.

$$\begin{aligned}\hat{H}|A_i\rangle &= 2u|A_i\rangle - t_\perp|D_{i,i}\rangle - I_{i>2}|C_{i-1,i}\rangle - I_{i\leq\frac{n}{2}}|C_{i,i+1}\rangle, \\ \hat{H}|B_i\rangle &= 2u|B_i\rangle - t_\perp I_{i>1}|D_{i,i}\rangle - I_{i>1}|E_{i-1,i}\rangle - I_{i\leq\frac{n}{2}}|E_{i,i+1}\rangle,\end{aligned}$$

where $I_K = 1$ if the statement K is true, and $I_K = 0$ otherwise.

The following three equations describe the action of \hat{H} on the basis wave vectors containing only one doubly occupied site ($|C_{i,j}\rangle, |D_{i,j}\rangle, |E_{i,j}\rangle$) as follows

$$\begin{aligned}\hat{H}|C_{i,j}\rangle &= \\ &u|C_{i,j}\rangle - 4\delta_{j,i+1}|A_i\rangle - 4\delta_{j,i+1}(1 + \delta_{i,\frac{n}{2}})|A_{i+1}\rangle - (1 - \delta_{i,2})|C_{i-1,j}\rangle \\ &- (1 - \delta_{j,i+1} - \delta_{i,2}\delta_{j,\frac{n+i}{2}+1})|C_{i,j-1}\rangle \\ &- (1 - \delta_{i,2}\delta_{j,\frac{n+i}{2}} + \delta_{j,n-i+1} - \delta_{j,n-i+2})|C_{i,j+1}\rangle \\ &- (1 - \delta_{j,i+1})(1 + \delta_{j,n-i+1} - \delta_{j,n-i+2})|C_{i+1,j}\rangle \\ &+ \delta_{i,2}(1 + \delta_{j,3})(1 - \delta_{j,\frac{n+i}{2}} - \delta_{j,\frac{n+i}{2}+1})|C_{2,n-j+3}\rangle \\ &- t_\perp|D_{i,j}\rangle - t_\perp \cdot \left\{ \begin{array}{l} I_{j\leq\frac{n}{2}+1}|D_{j,i}\rangle \\ I_{j>\frac{n}{2}+1}(1 - \delta_{j,n-i+2})|D_{n-j+2,n-i+2}\rangle \end{array} \right\} \\ &- (1 - \delta_{i,2})(1 + \delta_{j,i+1})|F_{i-1,i,n-j+i+1}\rangle \\ &+ \left\{ \begin{array}{l} (1 - \delta_{i,2})(1 + \delta_{j,i+1})(1 - \delta_{i,3}I_{j\geq\frac{n+i+1}{2}})|F_{i,2,j}\rangle \\ -\delta_{i,3}I_{j>\frac{n+i+1}{2}}|F_{i,2,n-j+i+1}\rangle \end{array} \right\} \\ &- (1 + \delta_{j,i+1})(1 + \delta_{j,n-i+1} - \delta_{j,n-i+2})|F_{i,i+1,n-j+i+1}\rangle\end{aligned}$$

$$\begin{aligned}
& + (1 + \delta_{j,i+1})(1 + \delta_{j,n-i+1} - \delta_{j,n-i+2}) \times \\
& \times \left\{ \begin{array}{l} (1 - \delta_{i,2} I_{j \geq \frac{n+i}{2}}) |F_{i+1,2,j+1}\rangle \\ -\delta_{i,2} I_{j > \frac{n+i}{2}} |F_{i+1,2,n-j+i+1}\rangle \end{array} \right\} + t_{\perp} \cdot \left\{ \begin{array}{l} -I_{j \leq \frac{n+i+1}{2}} |G_{i,j,1}\rangle \\ I_{j > \frac{n+i+1}{2}} |G_{i,n-j+i+1,i}\rangle \end{array} \right\} \\
& + t_{\perp} (1 - \delta_{j,n-i+2}) \cdot \left\{ \begin{array}{l} I_{j \leq \frac{n}{2}+1} \cdot \left\{ \begin{array}{l} I_{j < 2i-1} |G_{j,j-i+1,j}\rangle \\ -I_{j \geq 2i-1} |G_{j,i,1}\rangle \end{array} \right\} \\ I_{j > \frac{n}{2}+1} \cdot \left\{ \begin{array}{l} -I_{j \leq 2i-1} |G_{n-j+2,n-i+2,1}\rangle \\ I_{j > 2i-1} |G_{n-j+2,n-j+i+1,n-j+2}\rangle \end{array} \right\} \end{array} \right\}.
\end{aligned}$$

$$\hat{H}|D_{i,j}\rangle =$$

$$\begin{aligned}
& u|D_{i,j}\rangle - 4t_{\perp}\delta_{j,i}(|A_i\rangle + |B_i\rangle) \\
& - t_{\perp}(1 - \delta_{j,1} - \delta_{j,i} + \delta_{j,n-i+2}) \cdot \left\{ \begin{array}{l} I_{j \leq n-i+2} I_{j < i} (|C_{j,i}\rangle + |E_{j,i}\rangle) \\ I_{n-i+2 \geq j > i} (|C_{i,j}\rangle + |E_{i,j}\rangle) \\ I_{j > n-i+2} (|C_{n-j+2,n-i+2}\rangle + |E_{n-j+2,n-i+2}\rangle) \end{array} \right\} \\
& + \left\{ \begin{array}{l} -(1 - \delta_{i,2}) |D_{i-1,j}\rangle \\ \delta_{i,2} (1 - \delta_{j,1} - \delta_{j,2} - \delta_{j,\frac{n+i}{2}} - \delta_{j,\frac{n+i}{2}+1}) |D_{i,n+i-j+1}\rangle \end{array} \right\} \\
& - \left\{ \begin{array}{l} I_{j > 1} [1 - \delta_{i,2} (\delta_{j,2} + \delta_{j,\frac{n+i}{2}+1}) + \delta_{i,\frac{n}{2}+1} \delta_{j,2}] |D_{i,j-1}\rangle \\ \delta_{j,1} (1 - \delta_{i,\frac{n}{2}+1}) |D_{i,n}\rangle \end{array} \right\} \\
& - \left\{ \begin{array}{l} [1 - \delta_{i,2} (\delta_{j,1} + \delta_{j,\frac{n+i}{2}}) - \delta_{j,n} + \delta_{i,\frac{n}{2}+1} (\delta_{j,\frac{n}{2}} - \delta_{j,\frac{n}{2}+1})] |D_{i,j+1}\rangle \\ \delta_{j,n} |D_{i,1}\rangle \end{array} \right\} \\
& - \left\{ \begin{array}{l} [I_{i < \frac{n}{2}} + \delta_{i,\frac{n}{2}} (I_{j < \frac{n}{2}+1} + \delta_{j,1} + 2\delta_{j,\frac{n}{2}+1})] |D_{i+1,j}\rangle \\ (\delta_{i,\frac{n}{2}} I_{j > \frac{n}{2}+1} + \delta_{i,\frac{n}{2}+1} (1 - \delta_{j,1} - \delta_{j,i})) |D_{n-i+1,n-j+2}\rangle \end{array} \right\} \\
& - (1 - \delta_{i,2}) \left\{ \begin{array}{l} I_{j \leq i} |G_{i-1,i,i-j+1}\rangle \\ I_{j > i} |G_{i-1,i,n-j+i+1}\rangle \end{array} \right\} + \left\{ \begin{array}{l} [1 - \delta_{i,2} - \delta_{i,3} (\delta_{j,2} + \delta_{j,3} + I_{j > \frac{n}{2}+1})] |G_{i,2,j}\rangle \\ -\delta_{i,3} \delta_{j,3} |G_{i,2,1}\rangle \\ -\delta_{i,3} I_{j > \frac{n}{2}+2} |G_{i,2,n-j+i+1}\rangle \end{array} \right\} \\
& + \left\{ \begin{array}{l} (1 - \delta_{i,\frac{n}{2}+1}) \left\{ \begin{array}{l} -I_{j \leq i} |G_{i,i+1,i-j+1}\rangle \\ -I_{j > i} |G_{i,i+1,n+i-j+1}\rangle \end{array} \right\} \\ \delta_{i,\frac{n}{2}+1} I_{1 < j < \frac{n}{2}+1} (1 - \delta_{n,4} \delta_{j,2}) |G_{i,2,n-j+2}\rangle \end{array} \right\}
\end{aligned}$$

$$\begin{aligned}
& + \left\{ \begin{aligned} & [1 - \delta_{j,n} - \delta_{i,\frac{n}{2}+1} - \delta_{i,2}(\delta_{j,1} + \delta_{j,2} + I_{j \geq \frac{n}{2}+1})] |G_{i+1,2,j+1}\rangle \\ & \delta_{j,n} |G_{i+1,2,1}\rangle \\ & -\delta_{i,\frac{n}{2}+1} I_{1 < j < \frac{n}{2}+1} |G_{\frac{n}{2},\frac{n}{2}+1,\frac{n}{2}+j}\rangle \\ & -\delta_{i,2} \left\{ \begin{aligned} & \delta_{j,2} |G_{i+1,2,1}\rangle \\ & I_{\frac{n}{2}+1 < j < n} |G_{i+1,2,n+i-j+1}\rangle \end{aligned} \right\} \end{aligned} \right\} \\
& -t_{\perp} \cdot \left\{ \begin{aligned} & I_{1 < j < i} |H_{j,j,n-i+j+1}\rangle \\ & 4\delta_{i,j} |H_{j,j,1}\rangle \\ & (I_{i < j < n-i+2} + 2\delta_{j,n-i+2}) |H_{i,i,n-j+i+1}\rangle \\ & I_{j > n-i+2} |H_{n-j+2,n-j+2,n+i-j+1}\rangle \end{aligned} \right\} + t_{\perp} \cdot \left\{ \begin{aligned} & (I_{1 < j < i} + 4\delta_{j,i}) |J_{j,1,i}\rangle \\ & (1 - \delta_{j,i})(I_{i < j < n-i+2} + 2\delta_{j,n-i+2}) |J_{i,1,j}\rangle \\ & I_{j > n-i+2} |J_{n-j+2,1,n-i+2}\rangle \end{aligned} \right\}.
\end{aligned}$$

$$\hat{H}|E_{i,j}\rangle =$$

$$\begin{aligned}
& u|E_{i,j}\rangle - 4\delta_{j,i+1}[(1 + \delta_{i,1})|B_i\rangle + (1 + \delta_{i,\frac{n}{2}})|B_j\rangle] - t_{\perp}(1 - \delta_{i,1}) \cdot \left[|D_{i,j}\rangle \right. \\
& + \left. \left\{ \begin{aligned} & I_{j \leq \frac{n}{2}+1} |D_{j,i}\rangle \\ & I_{\frac{n}{2}+1 < j < n-i+2} |D_{n-j+2,n-i+2}\rangle \end{aligned} \right\} \right] - \left\{ \begin{aligned} & [1 - \delta_{i,1} + \delta_{i,2}(\delta_{j,\frac{n}{2}+1} - I_{j > \frac{n}{2}+1})] |E_{i-1,j}\rangle \\ & \delta_{i,2} I_{j > \frac{n}{2}+1} |E_{i-1,n-j+2}\rangle \\ & \delta_{i,1}(1 + \delta_{j,2} - \delta_{j,\frac{n}{2}+1}) |E_{2,n-j+2}\rangle \end{aligned} \right\} \\
& -(1 - \delta_{j,i+1}) |E_{i,j-1}\rangle - (1 + \delta_{j,n-i+1} - \delta_{j,n-i+2} + \delta_{i,1}\delta_{j,\frac{n}{2}} - \delta_{i,1}\delta_{j,\frac{n}{2}+1}) |E_{i,j+1}\rangle \\
& -(1 - \delta_{j,i+1})(1 + \delta_{j,n-i+1} - \delta_{j,n-i+2}) |E_{i+1,j}\rangle + t_{\perp}(1 - \delta_{i,1}) \cdot \left\{ \begin{aligned} & -I_{j \leq \frac{n+i+1}{2}} |G_{i,j,1}\rangle \\ & I_{j > \frac{n+i+1}{2}} |G_{i,n-j+i+1,i}\rangle \end{aligned} \right\} \\
& + t_{\perp}(1 - \delta_{i,1} - \delta_{j,n-i+2}) \cdot \left\{ \begin{aligned} & I_{j \leq \frac{n}{2}+1} \cdot \left\{ \begin{aligned} & I_{j < 2i-1} |G_{j,j-i+1,j}\rangle \\ & -I_{j \geq 2i-1} |G_{j,i,1}\rangle \end{aligned} \right\} \\ & I_{j > \frac{n}{2}+1} \cdot \left\{ \begin{aligned} & -I_{j \leq 2i-1} |G_{n-j+2,n-i+2,1}\rangle \\ & I_{j > 2i-1} |G_{n-j+2,n-j+i+1,n-j+2}\rangle \end{aligned} \right\} \end{aligned} \right\} \\
& + (1 + \delta_{j,i+1}) \cdot \left\{ \begin{aligned} & I_{i > 2} |H_{i-1,n-j+i+1,i}\rangle \\ & \delta_{i,2} |H_{1,2,n-j+i+1}\rangle \\ & \delta_{i,1} \cdot \left\{ \begin{aligned} & 2\delta_{j,2} |H_{2,2,1}\rangle \\ & I_{\frac{n}{2}+1 > j > 1} |H_{2,2,n-j+3}\rangle \end{aligned} \right\} \end{aligned} \right\} + [1 + \delta_{j,i+1}(1 + 2\delta_{i,1})] |H_{i,2,j}\rangle \\
& + \left\{ \begin{aligned} & I_{i > 1}(1 + \delta_{j,i+1})(1 + \delta_{j,n-i+1} - \delta_{j,n-i+2}) |H_{i,n-j+i+1,i+1}\rangle \\ & \delta_{i,1}(1 + \delta_{j,i+1} - \delta_{j,\frac{n}{2}+1}) |H_{1,2,n-j+i+1}\rangle \end{aligned} \right\} \\
& + (1 + \delta_{j,i+1})(1 + \delta_{j,n-i+1} - \delta_{j,n-i+2}) |H_{i+1,2,j+1}\rangle.
\end{aligned}$$

The last four equations devoted to the base vectors $|F_{i,j,k}\rangle, |G_{i,j,k}\rangle, |H_{i,j,k}\rangle, |J_{i,j,k}\rangle$ (not containing doubly occupied sites) can be find in Ref.[⁵⁹].

APPENDIX B: EXEMPLIFICATION FOR GROUND STATE WAVE FUNCTIONS

We present below the leading terms of explicit ground state wave functions deduced for $N = 28$, at $|U/t_{\parallel}| = 3$. The ground state $|\Psi_g\rangle$ is normalized to unity, and contains ortho-normalized basis wave vectors.

For $t_{\perp}/t_{\parallel} = 0.8$ one obtains for the ground state wave function

$$\begin{aligned}
|\Psi_g\rangle = & 0.181883|E_{7,8}\rangle + 0.181878|C_{7,8}\rangle + 0.175769|D_{7,7}\rangle + 0.169247|C_{6,7}\rangle \\
& + 0.169246|E_{6,7}\rangle + 0.157289|D_{6,6}\rangle + 0.145021|C_{5,6}\rangle + 0.145004|E_{5,6}\rangle \\
& + 0.138346|D_{8,7}\rangle + 0.138346|D_{7,8}\rangle + 0.128723|D_{6,7}\rangle + 0.128721|D_{7,6}\rangle \\
& + 0.12823|D_{5,5}\rangle + 0.111346|C_{4,5}\rangle + 0.111315|E_{4,5}\rangle + 0.110256|D_{5,6}\rangle \\
& + 0.110239|D_{6,5}\rangle + 0.10177|E_{6,8}\rangle + 0.101761|C_{6,8}\rangle + 0.097877|G_{7,8,1}\rangle \\
& - 0.0978768|G_{8,2,8}\rangle + 0.0931102|D_{7,9}\rangle + 0.0913856|D_{4,4}\rangle - 0.0910721|G_{7,2,7}\rangle \\
& + 0.0910714|G_{6,7,1}\rangle + 0.0909671|C_{5,7}\rangle + 0.0909645|E_{5,7}\rangle + 0.0898481|D_{8,6}\rangle \\
& + 0.0898458|D_{6,8}\rangle + 0.0845566|D_{4,5}\rangle + 0.0844776|D_{5,4}\rangle + 0.0802931|D_{5,7}\rangle \\
& + \dots,
\end{aligned} \tag{B1}$$

while for $t_{\perp}/t_{\parallel} = 0.1$ one has

$$\begin{aligned}
|\Psi_g\rangle = & 0.29866|E_{7,8}\rangle + 0.29365|E_{6,7}\rangle + 0.284039|E_{5,6}\rangle + 0.270726|E_{4,5}\rangle \\
& + 0.255311|E_{3,4}\rangle + 0.240496|E_{2,3}\rangle + 0.230556|E_{1,2}\rangle + 0.16658|C_{7,8}\rangle \\
& + 0.156952|C_{6,7}\rangle + 0.149053|E_{6,8}\rangle + 0.145317|E_{5,7}\rangle + 0.13942|E_{4,6}\rangle \\
& + 0.137923|C_{5,6}\rangle + 0.131927|E_{3,5}\rangle + 0.123835|E_{2,4}\rangle + 0.116908|E_{1,3}\rangle \\
& + 0.110056|C_{4,5}\rangle + 0.081715|C_{6,8}\rangle + 0.0755983|E_{6,9}\rangle + 0.0751106|H_{6,13,7}\rangle \\
& - 0.0750843|H_{7,2,9}\rangle + 0.0746358|C_{3,4}\rangle + 0.0744796|C_{5,7}\rangle + 0.0743108|E_{5,8}\rangle \\
& + 0.0740908|B_7\rangle - 0.073841|H_{5,13,6}\rangle - 0.0738214|H_{6,2,8}\rangle - 0.0722444|B_6\rangle \\
& + 0.0718117|E_{4,7}\rangle - 0.0713933|H_{5,2,7}\rangle - 0.0713921|H_{4,13,5}\rangle + 0.0693442|B_5\rangle \\
& + \dots
\end{aligned} \tag{B2}$$

-
- ¹ P. A. Maksym, H. Imamura, G. P. Mallon, H. Aoki, Jour. of Phys. **C12**, R299, (2000).
 - ² V. P. Kochereshko et al., Physica **E17**, 197, (2003).
 - ³ O. Halfpap, Annalen Der Physik **10**, 623, (2001).
 - ⁴ C. A. Sackett et al., Nature **404**, 256, (2000).
 - ⁵ T. P. Martin, Phys. Rep. **95**, 168, (1983).
 - ⁶ M. Greiner, O. Mandel, T. Esslinger, T. W. Hansch, I. Bloch, Nature **415**, 39, (2002).
 - ⁷ D. S. Petrov, Phys. Rev. Lett. **93**, 143201, (2004).
 - ⁸ D. McGloin, A. E. Carruthers, K. Dholakia, E. M. Wright, Phys. Rev. **E69**, 021403, (2004).
 - ⁹ M. Newey, J. Ozik, S. M. Van der Meer, E. Ott, W. Losert, Europhys. Lett. **66**, 205, (2004).
 - ¹⁰ J. E. Park, I. Jasiuk, A. Zubelewicz, Jour. of Electr. Packaging **125**, 400, (2003)
 - ¹¹ Y. Chen, A. T. Chwang, Jour. Engineering Mechanics ASCE. **129**, 1156, (2003).
 - ¹² V. Tikare, M. Braginsky, E. A. Olevsky, Jour. Amer. Ceram. Soc. **86**, 49, (2003).
 - ¹³ Zs. Gulácsi, M. Gulácsi, Phys. Rev. Lett. **73**, 3239, (1994).
 - ¹⁴ A. Amaya-Tapia, G. Gasaneo, S. Ovchinnikov, J. H. Macek, S. Y. Larsen, Jour. Math. Phys. **45**, 3533, (2004).
 - ¹⁵ A. I. Davydychev, R. Delbourgo, Jour. of Phys. **A37**, 4871, (2004).
 - ¹⁶ A. S. Kadyrov, A. M. Mukhamedzhanov, A. T. Stelbovic, I. Bray, F. Pirlepesov, Phys. Rev. **A68**, 022703, (2003).
 - ¹⁷ M. Sigrist, H. Tsunetsugu, K. Ueda, Phys. Rev. Lett. **67**, 2211, (1991).
 - ¹⁸ M. A. Khan, A. Pumar, J. C. Vassilicos, Phys. Rev. **E68**, 026313, (2003).
 - ¹⁹ A. O. Ivanov, S. S. Kantorovich, Colloid Jour. **65**, 166, (2003).
 - ²⁰ Y. Xu, K. D. Kafui, C. Thornton, G. P. Lian, Particle Sci. and Technol. **20**, 109, (2002).
 - ²¹ E. Kovács, Zs. Gulácsi, Phil. Mag. **B81**, 1557, (2001).
 - ²² U. Merkt, J. Huser, M. Wagner, Phys. Rev. **B43**, 7320, (1991).
 - ²³ L. Chen, C. Mei, Phys. Rev. **B39**, 9006, (1989).
 - ²⁴ C. Mei, L. Chen, Zeit. für Phys. **B72**, 429, (1988).
 - ²⁵ A. Parola, S. Sorella, M. Parinello, E. Tosatti, Phys. Rev. **B43**, 6190, (1991).
 - ²⁶ B. Szafran et al. Phys. Rev. **B70**, 235335, (2004).
 - ²⁷ A. Luis, Phys. Lett. **A314**, 197, (2003).

- ²⁸ A. Comtet, J. Desbois, Jour. of Phys. **A36**, L255, (2003).
- ²⁹ E. P. Nakhmedov, K. Morawetz, M. Ameduri, A. Yurtsever, C. Radehaus, Phys. Rev. **B67**, 205106, (2003).
- ³⁰ N. G. Zhang, C. L. Henley, Eur. Phys. Jour. **B38**, 409, (2004).
- ³¹ S. A. Mikhailov, Phys. Rev. **B66**, 153313, (2002).
- ³² G. Katomeris, F. Selva, J. L. Pichard, Eur. Phys. Jour. **B31**, 401, (2003); *ibid* **B33**, 87, (2003).
- ³³ X. R. Zhou, L. Guo, J. Meng, E. G. Zhao, Commun. in Theor. Phys. **37**, 583, (2002).
- ³⁴ C. G. Papadopoulos, Comp. Phys. Commun. **137**, 247, (2001).
- ³⁵ J. McKeever, J. R. Buck, A. D. Boozen, H. J. Kimble, Phys. Rev. Lett. **93**, 143601, (2004).
- ³⁶ Z. J. Ying, Y. Q. Li, S. J. Gu et al., Jour. Math. Phys. **43**, 5977, (2002).
- ³⁷ C. A. Traynor, J. B. Anderson, B. M. Boghosian, Jour. Chem. Phys. **94**, 3657, (1991).
- ³⁸ G. Kato, M. Wadati, Chaos Solitons and Fractals **12**, 993, (2001).
- ³⁹ D. A. Mazziotti, R. M. Erdahl, Phys. Rev. **A63**, 042113, (2001).
- ⁴⁰ H. T. Chen, D. H. Feng, Phys. Rep. **264**, 91, (1996).
- ⁴¹ O. A. Chubykalo, A. S. Kovalev, O. V. Usatenko, Phys. Lett. **A178**, 129, (1993).
- ⁴² Y. Uesaka, Y. Nakatani, N. Hayashi, Jour. Magn. Magn. Matter. **123**, 209, (1993).
- ⁴³ T. Okabe, H. Yamada, Modern Phys. Lett. **B18**, 269, (2004).
- ⁴⁴ A. K. Pati, Phys. Lett. **A322**, 301, (2004).
- ⁴⁵ Z. I. Abdullaev, Theor. and Mathem. Physics **123**, 483, (2000).
- ⁴⁶ F. E. Harris, A. M. Frolov, V. H. Smith, Int. Jour. Quant. Chem. **100**, 1086, (2004).
- ⁴⁷ J. S. Kim, D. Coffey, Phil. Mag. **B74**, 477, (1996).
- ⁴⁸ M. Letz, R. J. Goodin, Jour. of Phys. **C10**, 6931, (1998).
- ⁴⁹ J. O. Sofo, C. A. Balseiro, Phys. Rev. **B45**, 8197, (1992).
- ⁵⁰ M. Fabrizio, A. Parola, E. Tosatti, Phys. Rev. **B44**, 1033, (1991).
- ⁵¹ E. H. Lieb, in Proceedings of the XI-th International Congress of Mathematical Physics, Edited by D. Iagolnitzer, International Press, Paris, pp.392.
- ⁵² C. A. Sackett, et al. Nature **404**, 256, (2000).
- ⁵³ J. Bell, *Speakable and Unspeakable in Quantum Mechanics*, Cambridge Univ. Press, 1987.
- ⁵⁴ J. Bollinger, W. M. Itano, D. Wineland, D. Heinzen, Phys. Rev. **A54**, R4649, (1996).
- ⁵⁵ H. K. Lo, S. Popescu, T. Spiller (eds), *Introduction to Quantum Computation and Information*, World Scientific, Singapore, 1997.

- ⁵⁶ C. Yannouleas, U. Landman, cond-mat/0501612.
- ⁵⁷ O. G uhne, Phys. Rev. Lett. **92**, 117903, (2004).
- ⁵⁸ We note that the here deduced ground states are entangled in the sense that cannot be factorized into a product of single-particle wave functions, although the constituent particles are entirely distinct, see Ref.^[52].
- ⁵⁹ The complete set of equations can be found in the Appendix 8 of the PhD thesis of E. Kovacs available at <http://www.dtp.atomki.hu/ekovacs/thesis>
- ⁶⁰ Such property is present also in the case of the Bethe Ansatz as well.
- ⁶¹ The α_{trans} and α_{rot} angles can be connected to the momentum and angular momentum values in the ground state.
- ⁶² O. Julliet, F. Gulminelli, Phys. Rev. Lett. **83**, 160401, (2004).
- ⁶³ R. M. Noack, N. Bulut, D. J. Scalapino, M. G. Zacher, Phys. Rev. **B56**, 7162, (1997).

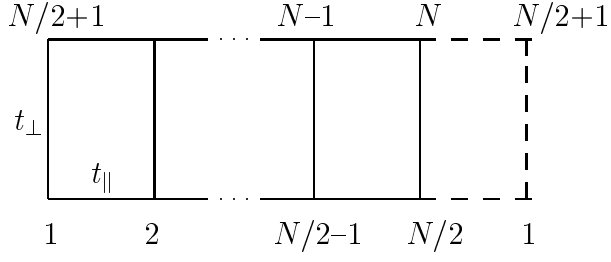


FIG. 1: The numbering of the lattice sites for the two leg ladder taken with periodic boundary conditions. N denoting the number of lattice sites is considered even. The t_{\perp} , (t_{\parallel}), denotes the inter-leg, (intra-leg) hopping matrix element.

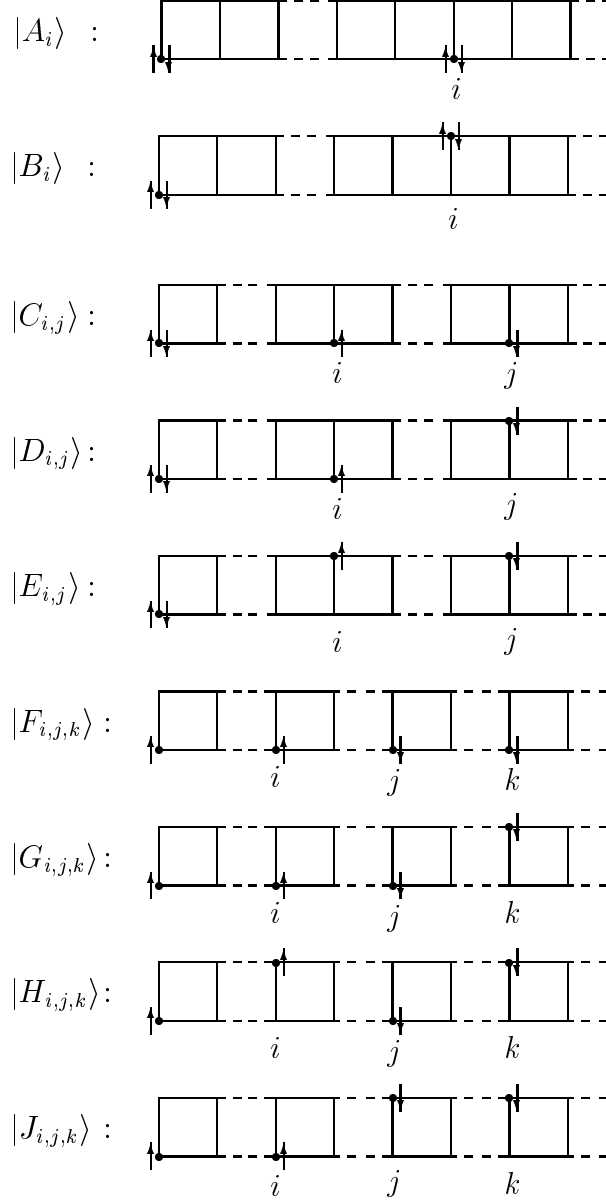


FIG. 2: The different possible types of base vectors. We note that for the cases C, E $i \neq j$, while for F, J $j < k$ is considered, respectively. In the cases F, G, H, J , the double occupancy is forbidden.

$$\begin{aligned}
& \left(\begin{array}{c} \text{Diagram 1} \\ \text{Diagram 2} \end{array} + \begin{array}{c} \text{Diagram 3} \\ \text{Diagram 4} \end{array} + \begin{array}{c} \text{Diagram 5} \\ \text{Diagram 6} \end{array} + \dots \right) + \\
& \left(\begin{array}{c} \text{Diagram 7} \\ \text{Diagram 8} \end{array} + \begin{array}{c} \text{Diagram 9} \\ \text{Diagram 10} \end{array} + \begin{array}{c} \text{Diagram 11} \\ \text{Diagram 12} \end{array} + \dots \right) + \\
& \left(\begin{array}{c} \text{Diagram 13} \\ \text{Diagram 14} \end{array} + \begin{array}{c} \text{Diagram 15} \\ \text{Diagram 16} \end{array} + \begin{array}{c} \text{Diagram 17} \\ \text{Diagram 18} \end{array} + \dots \right) + \\
& \left(\begin{array}{c} \text{Diagram 19} \\ \text{Diagram 20} \end{array} + \begin{array}{c} \text{Diagram 21} \\ \text{Diagram 22} \end{array} + \begin{array}{c} \text{Diagram 23} \\ \text{Diagram 24} \end{array} + \dots \right) + \\
& \left(\begin{array}{c} \text{Diagram 25} \\ \text{Diagram 26} \end{array} + \begin{array}{c} \text{Diagram 27} \\ \text{Diagram 28} \end{array} + \begin{array}{c} \text{Diagram 29} \\ \text{Diagram 30} \end{array} + \dots \right) + \\
& \left(\begin{array}{c} \text{Diagram 31} \\ \text{Diagram 32} \end{array} + \begin{array}{c} \text{Diagram 33} \\ \text{Diagram 34} \end{array} + \begin{array}{c} \text{Diagram 35} \\ \text{Diagram 36} \end{array} + \dots \right) + \\
& \left(\begin{array}{c} \text{Diagram 37} \\ \text{Diagram 38} \end{array} + \begin{array}{c} \text{Diagram 39} \\ \text{Diagram 40} \end{array} + \begin{array}{c} \text{Diagram 41} \\ \text{Diagram 42} \end{array} + \dots \right)
\end{aligned}$$

FIG. 3: The structure of the $|D_{2,3}\rangle$ base vector.

Figure caption for Fig.4:

The properties of the ground state for $t_{\perp} = t_{\parallel}$. (a) The dependence of the energy (in t_{\parallel} units) on $u = U/t_{\parallel}$. The continuous line is the total energy, while the dots indicate the potential energy. (b) The logarithm of the same-leg \hat{S}^z - \hat{S}^z correlation function for $u = 0$ (dots, dot-dashed line), $u = -10$ (squares, long dashed line), $u = -30$ (diamonds, short dashed line), $u = -100$ (stars, continuous line). (c) The same-leg density-density correlation function for $u = 0$ (dots, dot-dashed line), $u = -10$ (squares, long dashed line), $u = -30$ (diamonds, short dashed line), $u = -100$ (stars, continuous line).

Figure caption for Fig.5:

Superconducting ground state correlation functions. (a) The same-leg superconducting s-wave correlation function for $t_{\perp} = t_{\parallel}$ and $u = 0$ (dots, dot-dashed line), $u = -10$ (squares, long dashed line), $u = -30$ (diamonds, short dashed line), $u = -100$ (stars, continuous line). (b) The superconducting d-wave correlation function for $t_{\perp} = t_{\parallel}$ and $u = 0$ (dots, dot-dashed line), $u = -10$ (squares, long dashed line), $u = -30$ (diamonds, short dashed line), $u = -100$ (stars, continuous line). We mention that the curves corresponding to the last two u values are almost superposed. (c) Superconducting d-wave correlation function for $u = -10$ and $t = t_{\perp}/t_{\parallel}$ taken as $t = 1$ (squares, dot-dashed line), $t = 0.5$ (triangles, short dashed line), $t = 0.3$ (X-s, long dashed line), $t = 0.01$ (circles, continuous line).

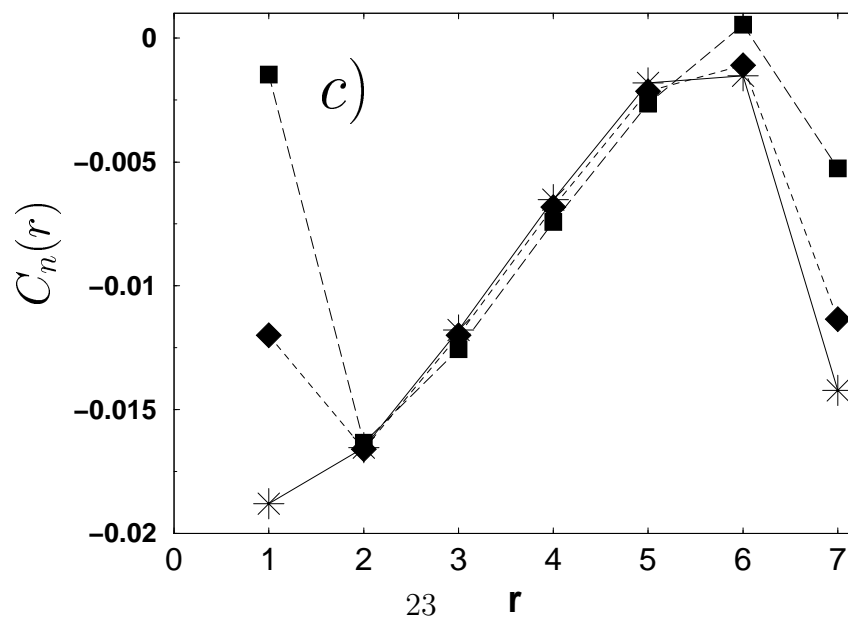
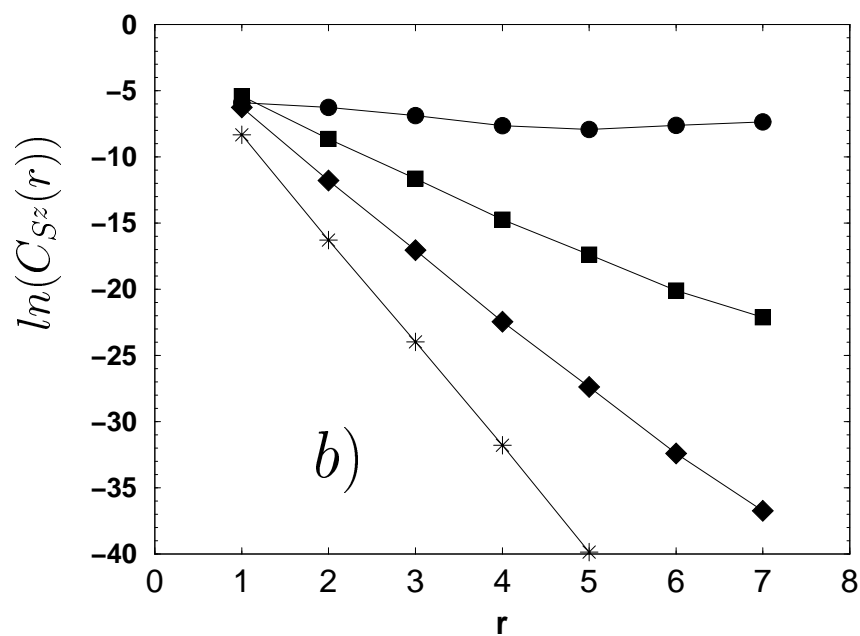
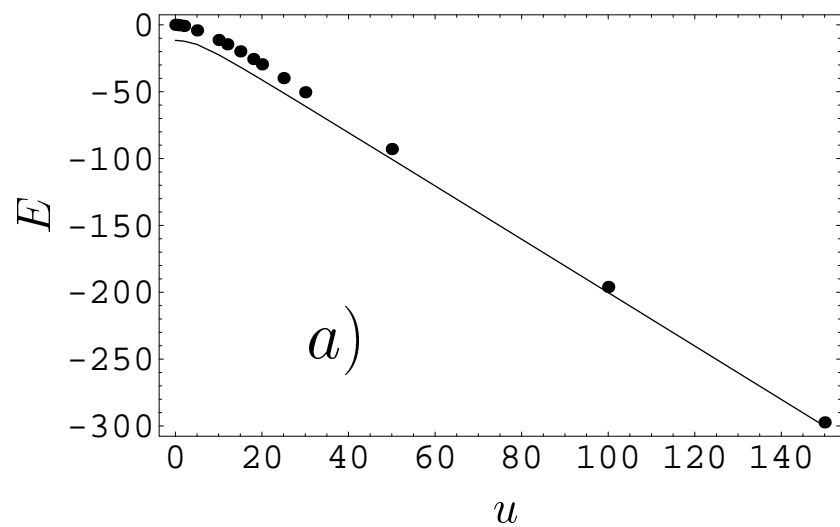


FIG. 4:

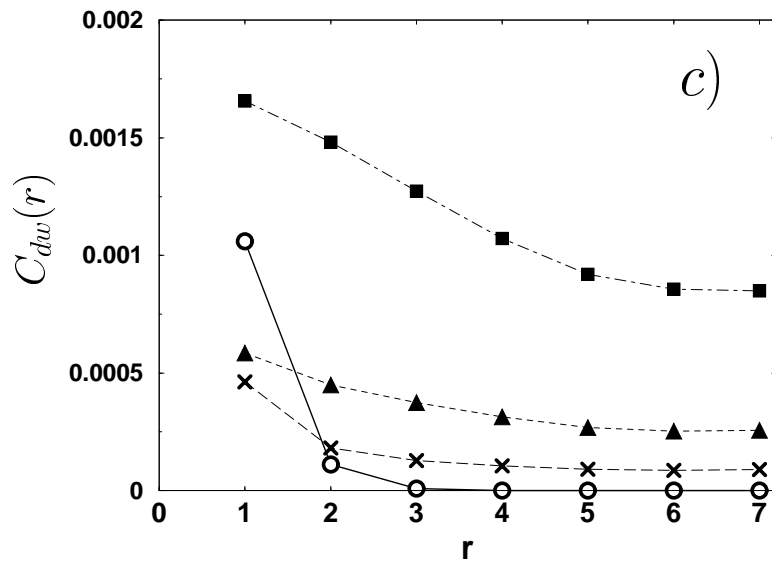
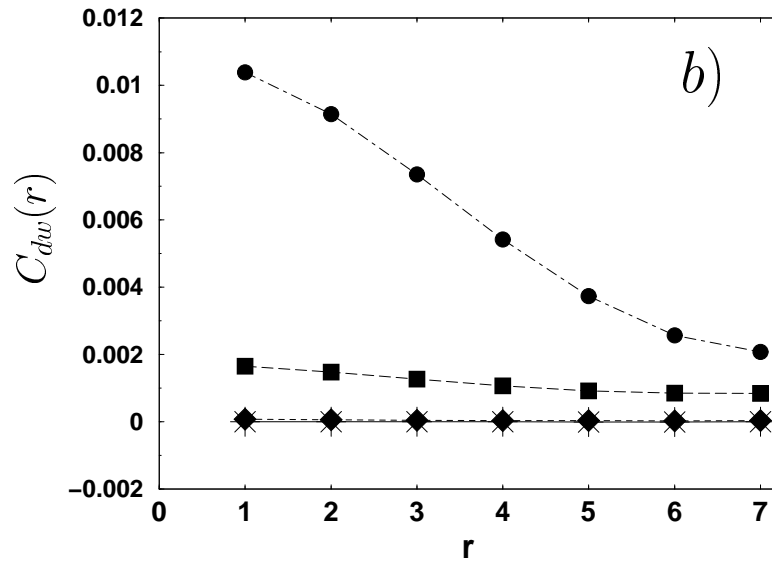
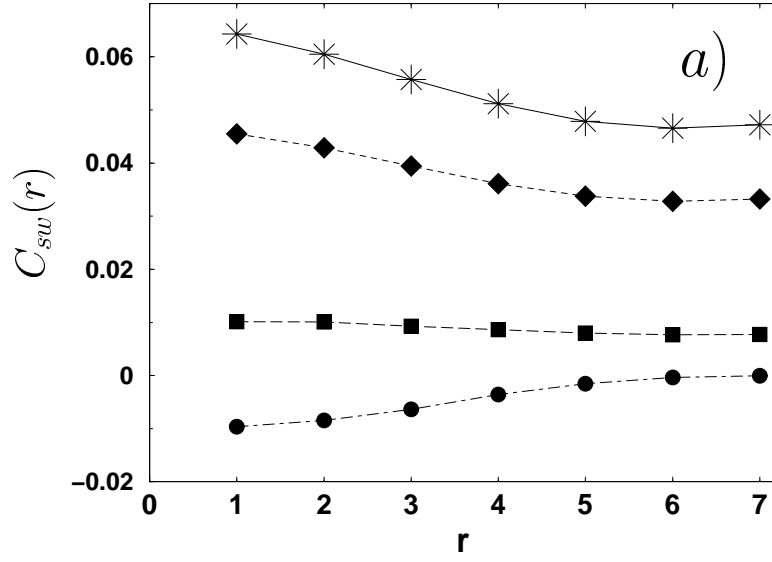


FIG. 5: